ELSEVIER

Biophysical Chemistry 71 (1998) 63–72

Biophysical Chemistry

A nanosecond fluorescence study of the simultaneous influx of Ca^{2+} and Cd^{2+} into liposomes

Kim Marie Hirshfield [a], Dmitri Toptygin [a], Gopal Grandhige [a], Beverly Z. Packard [b], Ludwig Brand [a,*]

[a] *Department of Biology, The Johns Hopkins University, Baltimore, MD 21218, USA*
[b] *OncoImmunin, 335 Paint Branch Drive, College Park, MD 20742, USA*

Received 19 June 1997; revised 27 November 1997; accepted 27 November 1997

Abstract

Nanosecond fluorescence decay characteristics of the calcium-binding probe Quin2 and two of its cation complexes were examined by time-resolved fluorescence spectroscopy. Binding of Ca^{2+} and Cd^{2+} resulted in fluorescence lifetime enhancements as compared to that of free Quin2 ($\langle\tau\rangle = 0.9$ ns). The Quin2–Ca^{2+} complex displays a monoexponential decay of $\tau = 7.4$ ns, while the cadmium complex gives an average decay time of ca. 4 ns. Lifetime measurements made on heterogeneous cationic solutions demonstrate that decay times for individual complexes can be retrieved. Time-resolved measurements were used to monitor the kinetics of ionomycin-mediated calcium and cadmium transport across artificial membranes. Fluorescence decays, collected on the time-scale of seconds, were sufficient to measure individual ion fluxes or those of mixtures into liposomes. The combination of steady-state and time-resolved fluorescence techniques offers the unique advantage of simultaneously detecting other cations in the presence of calcium. © 1998 Elsevier Science B.V.

Keywords: Fluorescence decay; Calcium transport; Cadmium transport; Time-resolved fluorescence spectroscopy

1. Introduction

Applications of fluorescence probes for quantitation of calcium in solution, model membranes, and living cells are well documented [1–10]. Fluorophores that chelate calcium including Quin-2, Fura-2, and Indo-1 have been of particular value [11,12]. Although some of the popular probes also bind to proteins with changes in spectroscopic properties, these signals can usually be differentiated from those associated with binding to calcium [13–15].

Spectroscopic probes can also be utilized to assay for other cations in biological systems [16–23]. For example, the deleterious toxicological effects of ions such as Pb^{2+} and Cd^{2+} have been investigated [17,20,23–26]. However, usually measurements of cations have been limited to the detection of individual ion species rather than to the measurement of multiple ions simultaneously. Previous attempts have been made to measure calcium and pH simultaneously using two different probes [27] while other efforts have focused on studying the movement of two cations with a single probe [17].

* Corresponding author. Department of Biology, The Johns Hopkins University, Mudd Hall, 3400 North Charles St., Baltimore, MD 21218, USA. Fax: +1-410-516-5213.

PII S0301-4622(97)00136-1

In order to develop a technique capable of monitoring multiple-ion movement, model liposome systems have been employed. The liposome-entrapped probes arsenazo III [28–31], Fura2 [9,32,33] and Quin2 [8,17], have been used previously to study calcium transport across artificial membranes. Ionophores such as ionomycin have been used to simulate cation fluxes since they insert into natural, as well as artificial membranes [7,32,33]. Fluorescence detection of multiple cations and their movement relies on the unique fluorescence characteristics produced by each cation complex. Measurements may be limited by data acquisition time, the ability to adequately resolve small changes as well as resolution of changes unique to cation concentration changes from other environmental perturbations.

Time-resolved fluorescence techniques are advantageous over steady-state fluorescence methods since they provide an additional dimension to the data and may be used to simultaneously detect multiple cations. The chemical system need not be perturbed by addition of other ions or chelators. For example, in work with some cell lines, steady-state fluorescence detection of calcium requires the addition of heavy metal chelators to remove Zn^{2+} which would otherwise interfere with the measured signals [34]. Cation complexes exhibiting unique fluorescence decay times can be resolved without perturbation of the intracellular milieu by addition of chelators. Methods that can identify and quantitate other cations in the presence of calcium also provide a relatively simple alternative to the use of radioactive isotopes [35,36]. Development of data acquisition and analysis associated with time-resolved techniques enables rapid data collection, e.g., on the time-scale of seconds, as well as increased resolution.

Quin2 possesses favorable fluorescence lifetime changes upon binding [37–42]. These changes can also be used to simultaneously monitor other cations using Quin2 or other fluorescent calcium chelating probes [39,41–49]. Additional information can be gained by the combination of steady-state and time-resolved fluorescence; the latter not only identifies cation complexes, but also provides a useful method for quantitation. In the present paper, we describe the use of nanosecond time-resolved fluorescence to investigate the kinetics of the ionomycin-mediated transport of calcium and cadmium into Quin2-loaded liposomes. This method demonstrates the value of time-resolved fluorescence to simultaneously measure multiple cation transport.

2. Materials and methods

2.1. Materials

Quin2 and 1-palmitoyl-2-oleyol-*sn*-glycero-3-phosphatidylcholine (POPC, purity > 99%) were purchased from Calbiochem (San Diego, CA). The source of Tris (ultrapure) was United States Biochemical (Cleveland, OH). EGTA, ethylenebis (oxynitrilo) tetraacetic acid, was obtained from Aldrich (St. Louis, MO). Cadmium chloride, zinc chloride, and calcium chloride were Baker-analyzed reagents. Calcium calibration buffers used for calcium titrations were obtained from Molecular Probes (Eugene, OR).

2.2. Liposome preparation

POPC, 130 mg, was hydrated in 10 mM Tris, pH 7.2, 5 mM Quin2, and 0.1 M KCl. To increase the Quin2-trapping efficiency, the lipid solution was frozen, thawed at 37°C, and vortexed [50,51]. The cycle was repeated four times. The lipid suspension was extruded using a 10-ml thermobarrel extruder from Lipex Biomembranes (Vancouver, BC) at 2100 kPa (350 psi) and 37°C. The barrel contained two Nucleopore 25 mm polycarbonate filters (0.1 μm) and a 25-mm PE drain disk. These extrusion procedures generated large unilamellar vesicles with relatively high dye-entrapping efficiencies [50–53]. Non-entrapped Quin2 was removed by passing the liposome preparation over a Sephadex PD10 (G25M) column which was pre-equilibrated with 10 mM Tris, pH 7.2, and 0.1 M KCl buffer. The liposomes were eluted from the column using the same buffer. The void volume of the column was 3 ml, determined by the elution of blue dextran. Non-entrapped Quin2 eluted from the column at approximately 9 ml. The first 2.4 ml of eluant was discarded. Eluant containing the Quin2-loaded liposomes was collected from 2.4 to 4.2 ml. This solution was diluted in 10 mM Tris, pH 7.2, 0.1 M KCl buffer for fluorescence measurements. Experiments were performed above

the lipid phase transition temperature (+3 to −5°C [54]).

2.3. Time-resolved fluorescence measurements

Fluorescence decay measurements were made using a time-correlated single photon counting instrument. The pulsed light source was a frequency-doubled output from a cavity-dumped dye laser, which was synchronously pumped by a frequency-doubled output from a mode-locked Nd:YAG laser (Spectra Physics Series 3000, Mountain View, CA). The dye laser contained DCM (4-(dicyanomethylene)-2-methyl-6-(*p*-dimethylaminostyryl)-4H-pyran; Kodak) dye to produce the desired excitation wavelength with optimal intensity. The dye laser was cavity-dumped at a frequency of 4 MHz. The cavity-dumped beam was frequency doubled to excite the sample at 325 nm. The frequency-doubled light passed through a Corning C7-54 filter to remove any light that was not frequency-doubled. The emission path contained a magic angle polarizer (54.7°), as well as an HT10 1200 vis grating monochromator (ISA Instruments SA, Edison, NJ) with 1 mm slits (8.5 nm spectral half bandwidth). Fluorescence emission was detected through both emission filters and a monochromator. The high degree of filtering provided by this combination resulted in no measurable scattered light component. Fluorescence was measured using a microchannel plate detector. The signal was electronically processed as described previously [55]. The functioning of the instrument was verified using an anthracene standard in ethanol ($\tau = 4.2$ ns). The sample holder and emission monochromator were under stepper motor control and allowed alternating measurements between a ludox scatterer ($\lambda_{em} = 325$ nm) and the sample ($\lambda_{em} = 490$ nm). The sample temperature was maintained using a Neslab TEQ temperature controller and PBC4 bath cooler.

2.4. Kinetic data acquisition and analysis

Kinetic fluorescence decay measurements on the time-domain instrument were made using the previously described kinetic collection program KINDK [56]. A total of 350 decay curves (2048 channels in each curve) were collected at 5-s intervals. Because of the short acquisition time, the amount of information contained in a single decay curve was insufficient to recover both lifetimes and preexponential factors; by the use of the global analysis, we overcame this problem. The data from all decay curves were fit simultaneously using the following model function:

$$R_m(t) = \Delta T_m^{(\text{live})} \times \sum_{i=1}^{N_{\text{sp}}} I_i(T_m) \times S_i(t) \qquad (1)$$

where t is the time after the laser pulse (nanosecond scale), T is the slow kinetic time-scale (in seconds), $R_m(t)$ is the decay curve collected during the interval from T_m to $T_m + \Delta T^{(\text{real})}$, $T_m = m \times 5$ s, $\Delta T^{(\text{real})} = 4.2$ s is the real time of data acquisition, $\Delta T_m^{(\text{live})}$ is the live time of data acquisition ($\Delta T_m^{(\text{live})}$ equals $\Delta T^{(\text{real})}$ less the dead time of the multichannel analyzer, 3.02 s $\leq \Delta T_m^{(\text{live})} \leq 3.72$ s), $N_{\text{sp}} = 3$ is the total number of species (Quin2, Quin2–Ca^{2+}, and Quin2–Cd^{2+}), I_i is the fluorescence intensity contributed by the species number i, and $S_i(t)$ is the decay of this species.

The decays of individual fluorescent species are the convolutions of the apparatus response function $A(t)$ with the δ-excitation decays $D_i(t)$:

$$S_i(t) = A(t) \otimes D_i(t) = \int_0^{\infty} A(t - t') \times D_i(t')\,\mathrm{d}t' \qquad (2)$$

The apparatus response function $A(t)$ contains contributions from the excitation pulse width, from the dispersion in the photon transit time in the emission monochromator, from the dispersion in the electron transit time in the microchannel plate photomultiplier, and from the noise in electrical amplifiers and discriminators. The apparatus response was determined experimentally prior to and after the fluorescence measurement using a scatterer in place of the fluorescence sample; the width of the apparatus response at half-maximum was 65 ps.

In order for every I_i in Eq. (1) to be the absolute fluorescence intensity, the functions $S_i(t)$ must be normalized to unit integrals,

$$\int_{-\infty}^{+\infty} S_i(t)\,\mathrm{d}t = 1$$

An integral from $-\infty$ to $+\infty$ of a convolution of two functions equals the product of integrals of the two functions. The function $A(t)$ was normalized to a unit integral, therefore the functions $D_i(t)$ also have to be normalized to unit integrals:

$$\int_0^\infty D_i(t)\,\mathrm{d}t = 1$$

For the species whose decay is single-exponential (such as Quin2–Ca^{2+}) the above normalization condition results in the preexponential multiplier $1/\tau_i$ (where τ_i is the lifetime),

$$D_i(t) = \frac{1}{\tau_i}\exp(-t/\tau_i)$$

For the species whose decay is multi-exponential (such as free Quin2) the following equation was used

$$D_i(t) = \sum_{j=1}^{n_i} \frac{f_{ij}}{\tau_{ij}}\exp(-t/\tau_{ij}) \qquad (3)$$

In Eq. (3), n_i is the number of exponentials associated with the species i, whereas τ_{ij} and f_{ij} are the lifetime and the fractional intensity contribution for the exponential number j. To satisfy the normalization condition, the sum of all fractional intensities corresponding to one component must equal unity. Eq. (3) can also be used for the species whose decay is single-exponential; in this case $n_i = 1$ and $f_{i1} = 1$.

The model function obtained by combining Eqs. (1)–(3) was used to simultaneously fit the family of 350 decay curves obtained in one kinetic experiment. The model function is linear in the $3 \times 350 = 1050$ local fitting parameters $I_{im} = I_i(T_m)$. In this work, we used the program L_GLOBAL, which takes advantage of the fact that the model function is linear in the local parameters I_{im} and nonlinear only in the global parameters f_{ij} and τ_{ij}, the count of which did not exceed 10. At each iteration the program expresses the linear parameters as functions of the nonlinear parameters, which reduces the dimensions of the Hessian matrix from 1060×1060 to 10×10. The time it takes to invert a matrix is proportional to the third power of its dimensions, therefore the gain in the speed of computations is $(1060/10)^3$, i.e., approximately a million times as compared to a regular nonlinear least-squares program.

The main outcome of the global analysis described above were the three functions $I_i(T)$, which describe the slow kinetics of the absolute fluorescence intensities associated with free Quin2 ($i = 1$), Quin2–Ca^{2+} ($i = 2$), and Quin2–Cd^{2+} ($i = 3$). In the absence of the inner-filter effect the fluorescence intensities $I_i(T)$ are proportional to the concentrations $C_i(T)$ of individual chemical species:

$$I_i(T) = P_i C_i(T) \qquad (4)$$

where the coefficients P_i are the products of five factors: the exciting power, the extinction coefficient of the species i at the exciting wavelength, the quantum yield of the species i, the shape of the emission spectrum of the species i, and the spectral sensitivity of the registration system. In Eq. (4) we implicitly assumed that none of these factors varies with time.

The system of Eq. (4) with $i = 1, 2, 3$ represents a system of three equations with three unknown coefficients and three unknown functions. If the total concentration of Quin2 is unknown, then the solution of this system is ambiguous. In the case where the total concentration is conserved in the course of one kinetic experiment, the solution can be made unambiguous by switching from the absolute concentrations $C_i(T)$ to fractional concentrations $F_i(T)$:

$$F_i(T) = C_i(T)/C_{\mathrm{TOT}} \qquad (5)$$

$$C_{\mathrm{TOT}} = \sum_{i=1}^{N_{\mathrm{sp}}} C_i(T) \qquad (6)$$

By introducing new coefficients $Q_i = 1/(C_{\mathrm{TOT}} \times P_i)$, Eq. (4) can be transformed to

$$F_i(T) = Q_i I_i(T) \qquad (7)$$

A combination of the system of Eq. (7) with the obvious constraint

$$\sum_{i=1}^{N_{\mathrm{sp}}} F_i(T) = 1 \qquad (8)$$

makes the solution unambiguous provided that the functions $I_i(T)$ are linearly independent. Note, that in the case of just two species, if the functions $I_i(T)$ change at all, then they are linearly independent. In

the case of three species, the functions $I_i(T)$ are linearly independent only if the concentrations of Ca^{2+} and Cd^{2+} inside liposomes are not changing proportionally to each other, i.e., if the diffusion coefficients for entry of the two ions into liposomes are different. The coefficients Q_i can be found by minimizing the sum

$$\mathrm{SSQ} = \sum_{m=1}^{N_{\mathrm{CURV}}} \left[1 - \sum_{i=1}^{N_{\mathrm{sp}}} Q_i I_i(T_m) \right]^2 \qquad (9)$$

The plain sum of squares SSQ in Eq. (9) was minimized using the method of linear least squares; the coefficients Q_i played the role of the optimized parameters. Once the coefficients Q_i were determined, they were used to calculate the fractional concentrations $F_i(T)$ using the system of equations (Eq. (7)).

The coefficients Q_i and P_i change when the total Quin2 concentration and/or the laser intensity changes; however, the proportions between these coefficients remain the same as long as the excitation wavelength, emission wavelength, temperature, and buffer composition remain unchanged. In this connection, it is convenient to define the ratios

$$E_i = \frac{P_i}{P_1} = \frac{Q_1}{Q_i} \qquad (10)$$

The ratios E_i will be referred to as the fluorescence enhancements upon binding Ca^{2+} (E_2) and Cd^{2+} (E_3). By definition, $E_1 = 1$, i.e., the fluorescence enhancement of free Quin2 equals unity. The fluorescence enhancements can be also measured in independent steady-state experiments, where saturating amounts of individual ions (either Ca^{2+} or Cd^{2+}) are added to the sample originally containing only free Quin2. In practice, however, such experiments might be difficult to carry out because of the background Ca^{2+} concentrations in deionized water and in the chemicals used in the buffer preparation.

3. Results and discussion

3.1. Time-resolved fluorescence of Quin2 and its cation complexes in solution

The steady-state fluorescence characteristics of Quin2, a chromophoric analog of the chelator EGTA, change upon cation chelation. Since fluorescence lifetimes are highly sensitive to probe environment, different cation complexes are expected to display unique decay times. Using instrumentation with nanosecond time resolution, one can separate the signals from individual ion complexes; this is not always possible with steady-state spectroscopy. Time-resolved fluorescence measurements of Quin2 have been described previously using frequency-domain [42,43] and time-domain instrumentation [37–41,49]. Fig. 1 depicts the fluorescence decay of Quin2 in the presence of calcium as measured with time-domain instrumentation. The intensity decay was well described by a monoexponential decay, $\tau = 7.4$ ns. A χ^2 of 1.1, together with the residuals and autocorrelation of the residuals as shown in Fig. 1, indicate that a monoexponential decay is an adequate fit for the fluorescence decay curve of the Quin2–Ca^{2+} complex.

The fluorescence decays of (a) free Quin2, (b) Quin2–Ca^{2+}, and (c) Quin2–Cd^{2+} at 37°C are shown in Fig. 2. In the absence of excited-state chemical reactions, the shape of the fluorescence decay of each fluorescent species is independent of the concentrations of Quin2 and the divalent ions; however, the relative concentrations of the three species depend on the concentrations of Quin2 and the ions. Under the conditions of Fig. 2, one species was present at a time. The visual differences between the observed decays for these complexes indicate that each complex displays a unique decay. Binding of Ca^{2+} and Cd^{2+} resulted in fluorescence lifetime enhancements as compared to that of free Quin2 ($\langle\tau\rangle = 0.9$ ns). The Quin2–Ca^{2+} complex displays a monoexponential decay of $\tau = 7.4$ ns while the cadmium complex gives an average decay time of ca. 4 ns.

3.2. Dynamic measurements of Quin2-loaded liposomes

Fluorescence lifetime measurements were made on Quin2-loaded POPC liposomes and those that were treated with calcium, cadmium, and ionomycin. Quin2 entrapment in lipid vesicles did not have any significant effects on its fluorescence properties. The intensity enhancements evoked by the addition of

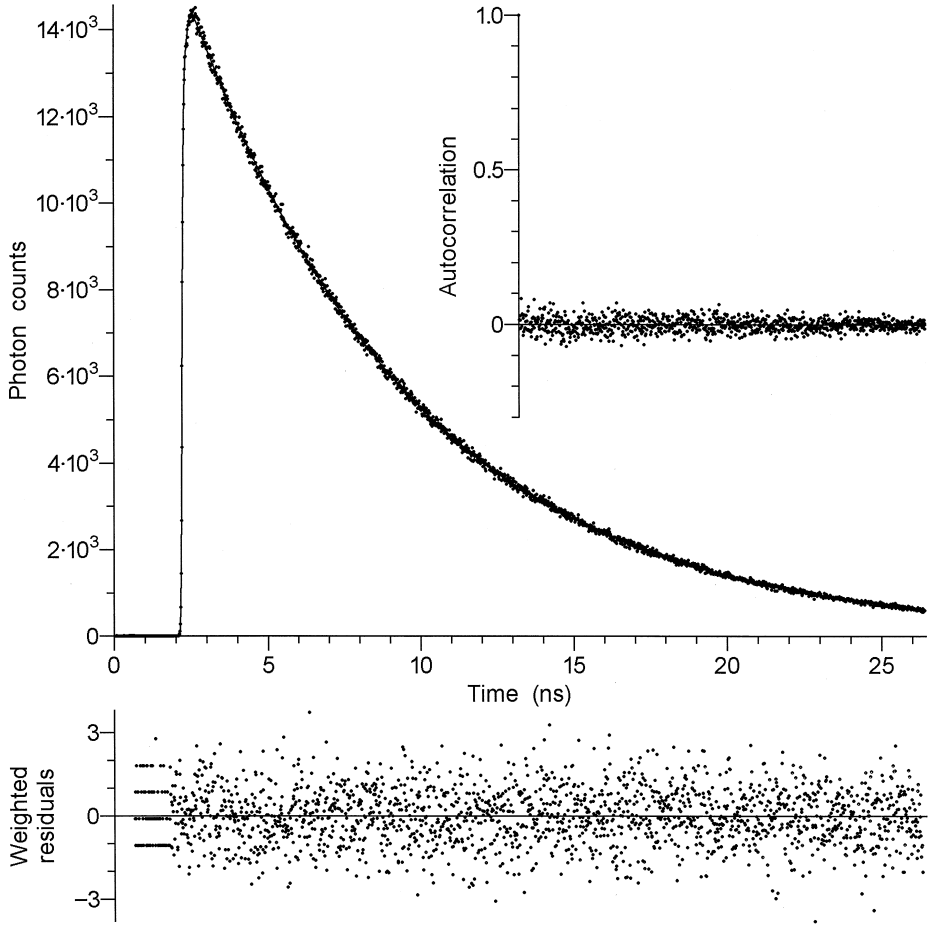

Fig. 1. Fluorescence decay of Quin2 in the presence of Ca^{2+} at 37°C: experimental data and fit by the convolution of a single exponential ($\tau = 7.4$ ns) with the apparatus response function of 65 ps (FWHM). The figure also shows weighted residuals and autocorrelation of residuals. The solution contained 17 μM Quin2, 150 mM Ca^{2+}, 100 mM KCl, and 10 mM Tris at pH = 7.2.

calcium and ionomycin to Quin2-loaded liposomes were the same as those seen in solution upon addition of calcium. Cation-specific lifetime changes were seen when both calcium and cadmium were added to Quin2-loaded liposomes. The ability to detect unique lifetimes made it possible to simultaneously monitor the movement of the two ions into the Quin2-loaded liposomes in the presence of ionomycin.

Since the Quin2–Ca^{2+} and Quin2–Cd^{2+} complexes display unique fluorescence decays compared to free Quin2, it was of interest to know if these spectral characteristics could be used to monitor the individual and simultaneous movement of calcium and cadmium into Quin2-loaded liposomes. To accomplish this, fluorescence decay curves were obtained at 5-s time intervals on Quin2-loaded liposomes as described in Section 2. The data were analyzed in terms of three components associated with free Quin2, Quin2–Ca^{2+} and Quin2–Cd^{2+}. The global analysis of the data set resulted in the reduced χ^2 of 0.976. Fig. 3 represents the changes in the *absolute intensity* contribution from each component. Initial measurements ($T = 0$) were made on Quin2-loaded liposomes alone. Calcium and cadmium were added to the liposome solution at $T = 100$ s, followed by addition of ionomycin at $T = 200$ s.

The initial decay curves collected on Quin2-loaded liposomes alone, indicate that the largest contributor

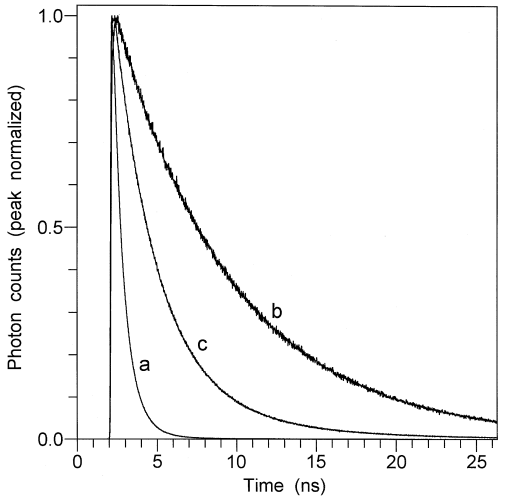

Fig. 2. Peak-normalized fluorescence decays of Quin2 at 37°C (a) in the absence of divalent ions, (b) in the presence of 150 mM Ca^{2+}, and (c) in the presence of 50 μM Cd^{2+}. The concentration of Quin2 equals 40 μM in (a) and (c) and 17 μM in (b).

to the fluorescence intensity is associated with free Quin2 (average lifetime = 0.9 ns). The nonzero intensity contribution from Quin2–Ca^{2+} observed before the addition of the ions to liposome solution is attributable to background levels of Ca^{2+} in the buffer solution. Since the intensity from the complex of Quin2 with the background Ca^{2+} is only 1/10 of the intensity of free Quin2, while the fluorescence intensity per mole of Quin2–Ca^{2+} is about 7 times greater than that per mole of free Quin2, the molar concentration of Ca^{2+}-bound Quin2 before the addition of the ions is only about 1.5%.

When the two cations are added in the absence of the ionophore to the liposomes at $T = 100$ s, there is a slight increase in the fluorescence intensity associated with the cadmium complex. There is also a small decrease in intensity associated with the free Quin2 component. This is due either to cadmium entering the liposomes, or to cadmium complexation with Quin2 located externally to the liposome membrane. Upon addition of ionomycin at $T = 200$ s, the intensity contribution from the calcium complex rises slowly until it reaches a peak of 18,500 photons/s by 500 s. Likewise, as the contribution from the calcium complex increases, there is an associated decrease in the intensity contribution of free Quin2. Curve (c) shows the appearance of intensity due to the Quin2–cadmium complex.

It is of interest that the total intensity increases after addition of ionomycin. The total intensity then declines after about 500 s. The cadmium complex has a lower fluorescence intensity per mole than does the calcium complex. The decreasing intensity is attributable to the competitive binding of cadmium to Quin2. There is clearly a change in the intensity contributions of each component as a function of time. The intensity of free Quin2 decreases as the signal due to the calcium and cadmium complexes increases. The intensity contributions for the cadmium complex increase throughout the time course of the experiment. The intensity contributions for the calcium complex rises initially and then declines as the emission of the cadmium complex dominates.

Fig. 4 indicates the changes in the *concentrations* of free Quin2, Quin2–Ca^{2+}, and Quin2–Cd^{2+} as a function of time after injection of Ca^{2+} and Cd^{2+} followed by injection of ionomycin as indicated by the arrows. Fluorescence intensities associated with specific species are proportional to the concentrations of these species, the coefficients of proportionality being different for different species. In order to calculate the fractional concentrations of different

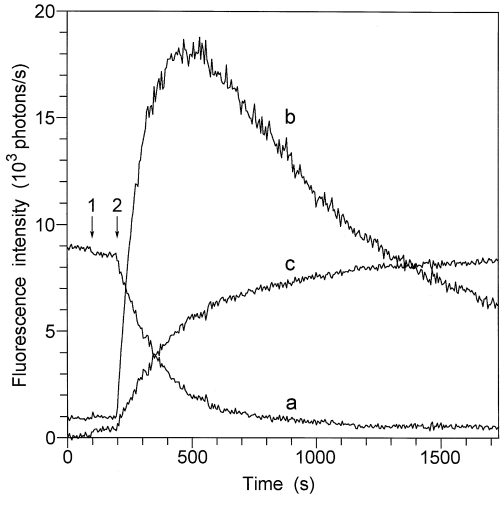

Fig. 3. Kinetics of fluorescence intensities of (a) free Quin2, (b) Quin2–Ca^{2+}, and (c) Quin2–Cd^{2+}. Arrows denote the injections of (1) $Ca^{2+} + Cd^{2+}$ and (2) ionomycin. Conditions described in text. [Ca^{2+}] = 15 mM, [Cd^{2+}] = 3.33 mM, and [ionomycin] = 4.3 μM.

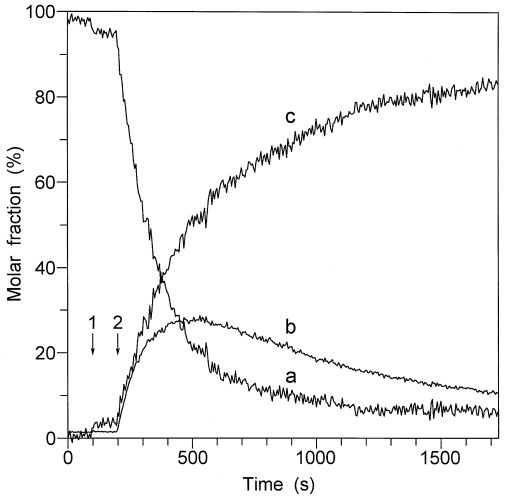

Fig. 4. Kinetics of molar fractions of (a) free Quin2, (b) Quin2–Ca^{2+}, and (c) Quin2–Cd^{2+}. Arrows denote the injections of (1) $Ca^{2+} + Cd^{2+}$ and (2) ionomycin.

forms of Quin2 at each time, we used the following equation:

$$F_i = \frac{I_i/E_i}{\sum_{j=1}^{3} I_j/E_j} \qquad (11)$$

where F_i is the fractional concentrations of the three forms of Quin2 ($i = 1$ for the free-form, $i = 2$ for the Ca^{2+}-bound form and $i = 3$ for the Cd^{2+}-bound form), I_i is the absolute fluorescence intensities associated with these forms, $E_1 = 1$, while $E_2 = 7.2$ and $E_3 = 1.2$, which denote fluorescence intensity enhancements resulting from the formation of Quin2–Ca^{2+} and Quin2–Cd^{2+} complexes. The kinetics of the fractional concentrations F_i calculated according to Eq. (11) is shown in Fig. 4.

The concentration of free Quin2 declines after addition of the ionophore while the concentrations of the cadmium and calcium complexes of Quin2 increase. The concentration of the calcium complex reaches a peak after about 500 s and then declines as the concentration of the Quin2–Cd^{2+} complex continues to increase.

Fig. 5 shows the fluorescence decay integrated over three different time windows of the cation influx kinetic experiment used to generate the data shown in Fig. 3. Curve (a) (Fig. 5) is dominated by the decay of free Quin2. Curve (b) has contributions from the decay of all three species and curve (c) is dominated by the decay of Quin2–Ca^{2+} and Quin2–Cd^{2+}. The integral under each decay curve shown in Fig. 5 equals the sum of the three intensities from Fig. 3 averaged over the appropriate time window and multiplied by the sum of the live times $T_m^{(\mathrm{live})}$ for the 20 decay curves corresponding to that time window.

In these experiments, fluxes of calcium and cadmium were monitored simultaneously. Although initially both ions appear to enter the liposomes and bind Quin2 at the same rate (Fig. 4), cadmium eventually causes release of Ca^{2+} from Quin2 by competitive binding. This may be due to a higher binding affinity of Quin2 for cadmium.

The process of ionomycin-mediated movement of cations is a diffusion-controlled process, i.e., it is governed by the concentration gradient across the bilayer. The 'kinetic endpoint' (equilibrium) will be reached when concentration of Ca^{2+} and Cd^{2+} is the same inside and outside the liposomes; at this concentration, there should be no free Quin2 left based on the large excess of the ions over Quin2. The results in Fig. 4 indicate that the concentration of free Quin2 does not approach zero at 1500 s after the addition of ionomycin. This points to the fact that

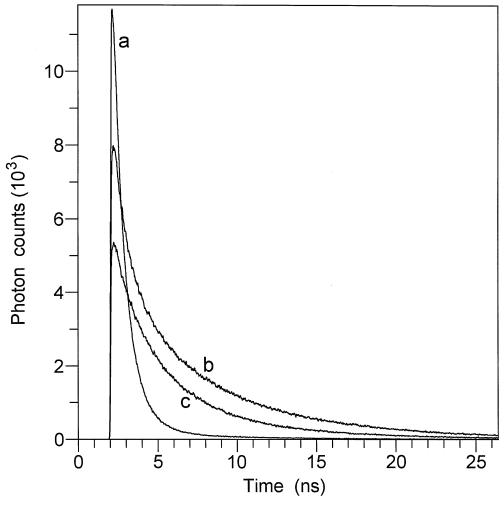

Fig. 5. Fluorescence decays of data shown in Figs. 3 and 4 integrated over the time windows of (a) 0–100 s, (b) 400–500 s, and (c) 1600–1700 s.

there is a sub-ensemble of vesicles, the diffusion of the cations into which is quite slow. On the other hand, the rapid build-up of Quin2–Ca^{2+} and Quin2–Cd^{2+} concentrations immediately after the addition of ionomycin reveals the presence of a sub-ensemble with a much faster diffusion rate. One may conclude that the permeability to Ca^{2+} and Cd^{2+} varies from vesicle to vesicle. This may be due to uneven distribution of ionomycin among vesicles and/or due to entrapment of smaller vesicles inside larger vesicles.

3.3. Conclusions

In this paper, we have shown that Quin2 can serve as an indicator for not only Ca^{2+}, but other cations, e.g., Cd^{2+}, by time-resolved fluorescence techniques. While time-resolved fluorescence techniques have been used previously to measure free and cation complexes in static situations, kinetic methods are capable of capturing the dynamics of such model systems. It is possible to measure single-cation movement across model membranes using the characteristic decay times associated with individual species. However, one goal is to use a single fluorescent probe to monitor a complex cationic milieu. The advantages of such a system would include simplification of mathematical calculations, since major ion species could be accounted for more accurately. The application of this method to intracellular measurements and other calcium-binding probes offers new possibilities for measuring multiple cation movement into liposomes and into cells.

Acknowledgements

We would like to acknowledge the initial contributions of John Wages to the time-resolved measurements with Quin2. We would also like to thank Dr. Robert DeToma for his development and construction of the sample collection apparatus of the time-domain instrumentation used in this work. Lastly, we appreciate the help from L.F. Hirshfield in the data collection. This work was taken in part from a PhD thesis submitted in partial fulfilment of the degree requirements in the Department of Biology at The Johns Hopkins University (K.M.H.). K.M.H. is supported by NIH Grant GM11632, NSF Grant DIR 8721059, and a gift from the W.M. Keck Foundation to The Institutes for Macromolecular Assemblies, The Johns Hopkins University. D.T. and L.B. are supported by NIH Grants GM07231 and GM11632.

References

[1] M.V. Thomas, Techniques in Calcium Research, Academic Press, New York, 1982.
[2] R.Y. Tsien, Methods in Cell Biology, Vol. 30, Academic Press, New York, 1989, pp. 127–157.
[3] R. Tsien, T. Pozzan, Methods Enzymol. 172 (1989) 230–262.
[4] R.Y. Tsien, Annu. Rev. Biophys. Bioeng. 12 (1983) 91–116.
[5] R.Y. Tsien, Annu. Rev. Neurosci. 12 (1989) 227–253.
[6] K.-Y. Nam, A. Morino, S. Kimura, H. Fujiki, Y. Imanishi, Biochem. J. 268 (1990) 169–173.
[7] C. Fasolato, T. Pozzan, J. Biol. Chem. 264 (1989) 19630–19636.
[8] S. Kimura, E. Ozeki, I. Imanishi, Biopolymers 28 (1989) 1235–1246.
[9] L. Blau, G. Weissman, Biochemistry 27 (1988) 5661–5666.
[10] J.P. Kao, Methods Cell Biol. 40 (1994) 155–181.
[11] R.Y. Tsien, Biochemistry 19 (1980) 2396–2404.
[12] G. Grynkiewicz, M. Poenie, R.Y. Tsien, J. Biol. Chem. 260 (1985) 3440–3450.
[13] E. Chiacone, E. Thulin, A. Boffi, S. Forsén, M. Brunori, J. Biol. Chem. 261 (1986) 16306–16308.
[14] J.R. Jefferson, J.B. Hunt, A. Ginsburg, Anal. Biochem. 187 (1990) 328–336.
[15] K.M. Hirshfield, D. Toptygin, G. Grandhige, H. Kim, B.Z. Packard, L. Brand, Biophys. Chem. 62 (1996) 25–38.
[16] C.-Y. Kwan, J.W. Putney, J. Biol. Chem. 265 (1990) 678–684.
[17] P.M. Hinkle, E.D. Shanshala, E.J. Nelson, J. Biol. Chem. 267 (1993) 25553–25559.
[18] E.B. Jones, D.J. Nelson, M.M. Turnbull, J. Inorg. Biochem. 45 (1992) 85–92.
[19] C.S. Owen, N.L. Sykes, R.L. Shuler, D. Ost, Anal. Biochem. 192 (1991) 142–148.
[20] J.L. Tomsig, J.B. Suszkiw, Am. J. Physiol. 259 (1990) C762–C768.
[21] R.D. Grubbs, M.E. Maguire, J. Biol. Chem. 261 (1986) 12550–12554.
[22] J.E. Merritt, T.J. Hallam, J. Biol. Chem. 263 (1988) 6161–6164.
[23] M. Nordberg, Environ. Rev. 15 (1978) 381–404.
[24] L. Friberg, Environ. Health Perspect. 54 (1984) 1–11.
[25] Z.A. Shaikh, L.M. Smith, Experientia Suppl. (1986) 124–130.
[26] M. Costa, Metal Carcinogenesis Testing, Humana Press, Clifton, NJ, 1980, pp. 25–35.
[27] G.T. Rijkers, L.B. Justement, A.W. Griffioen, J.C. Cambier, Cytometry 11 (1990) 923–927.
[28] P.M. Sokolove, M.B. Kester, Anal. Biochem. 177 (1989) 402–406.

[29] V.S. Ananthanarayanan, L.B. Taylor, S. Pirritano, Biochem. Cell Biol. 70 (1992) 608–612.
[30] H. Ramos, A. Attias de Murciano, B.E. Cohen, J. Bolard, Biochim. Biophys. Acta 982 (1989) 303–306.
[31] M.B. Kester, P.M. Sokolove, Biochim. Biophys. Acta 980 (1989) 127–133.
[32] P.W. Reed, H.A. Lardy, J. Biol. Chem. 247 (1972) 6970–6977.
[33] B.C. Pressman, M. Fahim, Annu. Rev. Pharmacol. Toxicol. 22 (1982) 465–490.
[34] P. Arslan, F. DiVirgilio, M. Beltrame, R.Y. Tsien, T. Pozzan, J. Biol. Chem. 260 (1985) 2719–2727.
[35] C.D. Ferris, R.L. Huganir, S. Supattapone, S.H. Snyder, Nature 342 (1989) 87–89.
[36] P. Grasso, T.A. Santa-Coloma, L.E. Reichert, Endocrinology 128 (1991) 2745–2751.
[37] J. Wages, B.S. Packard, D. Walbridge, L. Brand, J. Cell Biol. 103 (1986) 514A.
[38] J. Wages, B.S. Packard, M. Edidin, L. Brand, Biophys. J. 51 (1987) 284A.
[39] K.M. Hirshfield, L. Brand, Abstr. 10th Int. Biophys. Congr. 123 (1990) 1.8.19.
[40] N. Miyoshi, K. Hara, S. Kimura, K. Nakanishi, Photochem. Photobiol. 53 (1991) 415–418.
[41] K.M. Hirshfield, B.S. Packard, L. Brand, Biophys. J. 61 (1992) 1803.
[42] J.R. Lakowicz, H. Szmaczinski, K. Nowaczyk, M.L. Johnson, Cell Calcium 13 (1992) 131–147.
[43] K.M. Hirshfield, D. Toptygin, B.Z. Packard, L. Brand, Anal. Biochem. 209 (1993) 209–218.
[44] H. Szmacinski, I. Gryczynski, J.R. Lakowicz, Biophys. J. 70 (1996) 547–555.
[45] I. Gryczynski, H. Szmacinski, J.R. Lakowicz, Photochem. Photobiol. 62 (1995) 804–808.
[46] H. Szmacinski, J.R. Lakowicz, Cell Calcium 18 (1995) 64–75.
[47] J.R. Lakowicz, H. Szmacinski, K. Nowaczyk, W.J. Lederer, M.S. Kirby, M.L. Johnson, Cell Calcium 15 (1994) 7–27.
[48] H. Szmacinski, I. Gryczynski, J.R. Lakowicz, Photochem. Photobiol. 58 (1993) 341–345.
[49] K.M. Hirshfield, D. Toptygin, B.Z. Packard, L. Brand, Biophys. J. 64 (1993) A162.
[50] L.D. Mayer, M.B. Bally, M.J. Hope, P.R. Cullis, Chem. Phys. Lipids 40 (1986) 333–345.
[51] C.J. Chapman, W.E. Erdahl, R.W. Taylor, D.R. Pfeiffer, Chem. Phys. Lipids 60 (1991) 201–208.
[52] F. Szoka, D. Paphadjopoulis, in: C.G. Knight (Ed.), Liposomes: From Physical Structure to Therapeutic Applications, Elsevier/North Holland Biomedical Press, NY, 1981, pp. 51–82.
[53] R. Nayar, M.J. Hope, P.R. Cullis, Biochim. Biophys. Acta 986 (1989) 200–206.
[54] J.R. Silvias, Thermotropic phase transitions of pure lipids in model membranes and their modifications by membrane proteins, in: P.C. Jost, O.H. Griffith (Eds.), Lipid–Protein Interactions, Wiley-Interscience, New York, pp. 239–281.
[55] M. Badea, L. Brand, Methods Enzymol. 61 (1979) 378–425.
[56] D. Walbridge, J.R. Knutson, L. Brand, Anal. Biochem. 161 (1987) 467–478.